

A comparison of the spectral energy and enstrophy budgets of blocking versus nonblocking periods

By ANTHONY R. HANSEN, *Department of Geology and Geophysics, Yale University, P.O. Box 6666, New Haven, Connecticut 06511, U.S.A.* and ALFONSO SUTERA, *Center for the Environment and Man, Inc., Hartford, Connecticut 06230, U.S.A.*

(Manuscript received October 18, 1982; in final form March 7, 1983)

ABSTRACT

The time mean spectral energy and enstrophy budgets for blocking versus nonblocking periods from the winters of 1978–79 and 1976–77 are calculated. The major differences in the 1978–79 cases were in the nonlinear interaction terms. A pronounced upscale cascade of kinetic energy and enstrophy from intermediate to planetary-scale wavenumbers during blocking was found. During December 1976, the energy and enstrophy budgets of a case of Atlantic blocking were very similar to the cases in 1978–79, but quite different from the persistent, greatly amplified, planetary-wave pattern that followed in January and February 1977 (as identified by Charney et al., 1981). Planetary-scale baroclinic processes were greatly increased during the 1977 event along with reduced intermediate-scale baroclinic activity and the absence of the upscale enstrophy cascade noted in the other blocking cases.

The predictability time (Lilly, 1970) based on the enstrophy flux function showed an increased predictability for the January–February 1977 event but no significant differences between the other blocking cases compared to the nonblocking sample. However, the reversal of the low wavenumber enstrophy cascade during blocking does suggest that blocking may be more persistent (due to reduced dissipation of the large-scale circulation) and therefore more predictable.

1. Introduction

The term “blocking” has been used to describe a variety of circulation features with characteristic time scales larger than the synoptic time scale. The importance of blocking events in causing extremes in local surface weather and the expectation that the existence of these persistent features would allow greater forecasting skill in numerical weather prediction models has stimulated a great deal of interest in them in recent years.

Diagnostic calculations have usually identified blocking with large-scale baroclinic processes (e.g., Paulin, 1970; Murakami and Tomatsu, 1965). Recently, Hansen and Chen (1982) were able to identify the initiation of two cases of blocking with enhanced baroclinic energy conversions. In one

case, intense baroclinic cyclone waves forced the development of a blocking high through nonlinear interactions. In the other case, large-scale baroclinic processes accompanied the block's development.

In the present study, we will attempt to identify any systematic differences in the time mean spectral energy and enstrophy budgets of blocking events compared to nonblocking periods using data from two recent winters (1976–77 and 1978–79). Recently, Bengtsson (1981) has shown from numerical simulations that during a blocking event the atmosphere is in general more predictable than during nonblocking periods.

We are interested to see whether any diagnostic evidence exists for the greater predictability of blocking found by Bengtsson. Although our sample

sizes are fairly small, several interesting features related to differences in the nonlinear interaction terms appear.

2. Procedures

2.1. Data

The data used in the study are the output of the twice daily operational analysis of the National Meteorological Center (NMC) from the winters (DJF) of 1976-77 and 1978-79. Data for the horizontal wind (u, v), geopotential height (z) and temperature (T) on a $2.5^\circ \times 2.5^\circ$ grid at the ten mandatory levels in the troposphere (1000, 850, 700, 500, 400, 300, 250, 200, 150 and 100 mb) were used. Vertical velocities calculated from the quasi-geostrophic ω equation (assuming $\omega = 0$ at 1000 and 100 mb) were used in the energetics calculation (Chen *et al.*, 1981). Fourier coefficients of u, v, z, T and ω were computed for every 2.5° of latitude at the 10 levels with the wavenumber expansion of these variables truncated after zonal wavenumber 18.

During 1976-77, NMC employed the analysis scheme of Flattery (1971) in which only the rotational component of the wind is retained in u and v . In 1978-79, a multivariate, optimum interpolation analysis scheme was employed (Bergman, 1979). In this case a small divergent component of the horizontal wind is retained. However, the kinetic energy content of this divergent wind is quite small (Chen and Tribbia, 1981) and we do not feel that it will adversely affect the evaluation of the vorticity advection terms in the enstrophy budget calculation (see below).

2.2 Analysis

In the interest of brevity, the spectral energetics and spectral enstrophy equations will be presented in symbolic form only. The formulation of the spectral energetics equations can be found in Saltzman (1957, 1970) and the formulation of the spectral enstrophy equations can be found in Chen and Tribbia (1980). Note that derivation of the enstrophy equations requires that we assume the wind field to be nondivergent. The 1978-79 NMC wind field is not nondivergent, as mentioned earlier, but we feel the advection of vorticity by the divergent component of the wind will be small compared to advection by the rotational

component and, therefore, the inclusion of a small divergent component in the horizontal wind will not affect our calculation.

The rates of change of wavenumber m kinetic energy (K_m), available potential energy (A_m) and enstrophy (E_m) are given by:

$$\frac{\delta}{\delta t} K_m = C(K_z, K_m) + C(A_m, K_m) + C_x(m|n, l) + B(K_m)$$

$$\frac{\delta}{\delta t} A_m = C(A_z, A_m) - C(A_m, K_m) + C_x(m|n, l) + G(A_m) + B(A_m)$$

and

$$\frac{\delta}{\delta t} E_m = C(E_z, E_m) + C_x(m|n, l) + \beta_m + G(E_m) + B(E_m).$$

Here, a z subscript denotes a zonal mean quantity

$$(\)_z = \frac{1}{2\pi} \int_0^{2\pi} (\) d\lambda \quad \text{where } \lambda = \text{longitude},$$

and an m subscript denotes a departure from this mean for wavenumber m . The notation $C(A, B)$ represents a conversion of energy (or enstrophy) from reservoir A to reservoir B . $C_x(m|n, l)$ denotes the rate of increase of the quantity X (where $X = K, A$ or E) at wavenumber m due to nonlinear triad interactions with all possible combinations of wavenumbers n and l . β_m represents the so-called β -effect ($-\mathbf{v} \cdot \nabla f$) in the enstrophy budget. We were unable to calculate the generation terms ($G(A_m)$ and $G(E_m)$) with available data. $B(X)$ denotes boundary flux terms due to fluxes of X across both vertical and horizontal boundaries.

We integrated the budget equations over the region from 30° N to 80° N and from 1000 mb to 100 mb. When not integrated over the entire mass of atmosphere, the budget equations include certain horizontal and vertical flux terms (Saltzman, 1970; Chen and Tribbia, 1980). With our data, we were unable to calculate the vertical flux terms, although the vertical fluxes could in principle, be competitive with the other terms. The horizontal flux terms are frequently small (except the flux of geopotential energy) and differences in them between blocking and nonblocking situations were

usually not significant. Therefore, we will not discuss them.

2.3. Selection of blocking days

Traditionally, blocking has been identified subjectively according to certain kinematic properties of the flow as set down by Rex (1950). Recently, blocking events have been identified as persistent departures from the climatological mean height field (Dole, 1978; Charney et al., 1981). Our primary goal is to study persistent, large-scale blocking events compared to predominantly zonal circulations and to eliminate short duration (synoptic time scale), low amplitude, small-scale features from our sample of blocking observations. Therefore, we restrict ourselves to cases of stationary or slowly propagating ridges where the departure of the 500 mb height from the zonal mean, averaged over every 2.5° of latitude from 55°–80° N, exceeded 250 m for seven days or more. Blocking events so selected were compared with the twice-daily NMC 500 mb charts. The correspondence between the dates of blocking events identified subjectively from the charts and those determined from persistent height departures was quite good. Discrepancies of one or two observations (12–24 hours) at most occurred at the beginning and ending of the individual blocking events. Frequently, the two selections were identical. Therefore the blocking days identified from the height departures were used to form the sample of blocking and nonblocking days. Any observation not falling in a blocking period was included in the nonblocking sample. We should note that chang-

ing one or two observations at the beginning or ending of a given blocking event from the blocking sample to the nonblocking sample (or vice versa) did not significantly affect the mean energy and enstrophy budgets.

In addition, a case of very large negative height departures occurred during January and February 1977. This particular event has been discussed in a number of contexts by numerous other authors. Its existence is correlated with a simultaneous, very cold sea surface temperature anomaly in the North Pacific Ocean (Miyakoda and Rosati, 1982). Charney et al. (1981) provide the dates of the two periods during January and February 1977 of the largest negative height departures from the climatological mean. We will use their dates for the persistent low height anomalies in our diagnostic calculation. In fact, these low anomalies persisted throughout most of January and February 1977 (Chen and Shukla, 1983). Because of the existence of large amplitude features of one type or another throughout the 1976–77 winter, no nonblocking days from this winter were included in our nonblocking sample. A summary of the blocking and nonblocking days for the two winters is given in Table 1.

Our selection procedure is admittedly arbitrary but it does identify periods of large persistent height departures. The comparison of these periods with synoptic charts indicates that these periods satisfy (for the most part) the conventional, subjective definition of blocking. However, the inherent subjectivity in identifying what does or does not constitute blocking continues to be a problem in diagnostic studies of the phenomenon.

Table 1. *Tabulation of blocking and nonblocking days from the 1978–79 and 1976–77 winters determined from persistent height departures (see text). Dates for the negative height anomalies in January–February 1977 were determined by Charney et al. (1981) as extreme departures from the climatological mean height*

1978–79

Blocking days (90 observations)

1. 0000 GMT 1 Dec.–1200 GMT 7 Dec.: Atlantic
2. 0000 GMT 20 Dec.–1200 GMT 27 Dec.: Atlantic
3. 1200 GMT 29 Dec.–0000 GMT 10 Jan.: Pacific
4. 0000 GMT 14 Jan.–1200 GMT 26 Jan.: Atlantic
5. 0000 GMT 16 Feb.–0000 GMT 22 Feb.: Atlantic

1976–77

Blocking days (36 observations)

1. 1200 GMT 11 Dec.–0000 GMT 29 Dec.: Atlantic

Nonblocking days (85 observations)

- 0000 GMT 8 Dec.–1200 GMT 19 Dec.
- 0000 GMT 28 Dec.–1200 GMT 28 Dec.
- 1200 GMT 10 Jan.–1200 GMT 13 Jan.
- 0000 GMT 27 Jan.–1200 GMT 15 Feb.
- 1200 GMT 22 Feb.–1200 GMT 28 Feb.

Charney et al. (1981) negative anomalies (76 observations)

1. 30 December–17 January
 2. 2 February–22 February
-

3. Results

3.1. 1978-79 winter

From December 1978 through February 1979, we identified five major blocking events, four over the Atlantic-European region and one over the North Pacific (Table 1). In general, the mean energy and enstrophy budgets of the Atlantic cases were similar to the Pacific case even though the initiation of the Pacific case was different from the late December 1978 case (Hansen and Chen, 1982). Whether or not the energetics of the Pacific case are typical of other Pacific blocking cases is unknown, although all the Atlantic events showed similar characteristics and were similar to the December 1976 case (see below). First, consider the average kinetic energy (K), enstrophy (E) and available potential energy (A) spectra (Fig. 1) of all five cases compared to the nonblocking days. In the mean, the kinetic energy in the longest waves

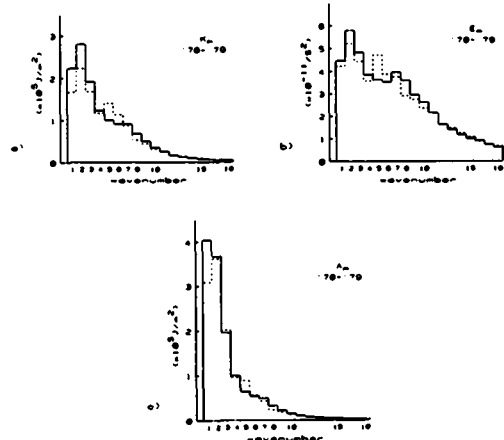


Fig. 1. Wavenumber spectra of (a) the kinetic energy, K_m ; (b) the enstrophy, E_m ; and (c) the available potential energy, A_m , for the 1978-79 winter. The solid line represents the mean spectra for all blocking days and the dashed line represents the nonblocking days.

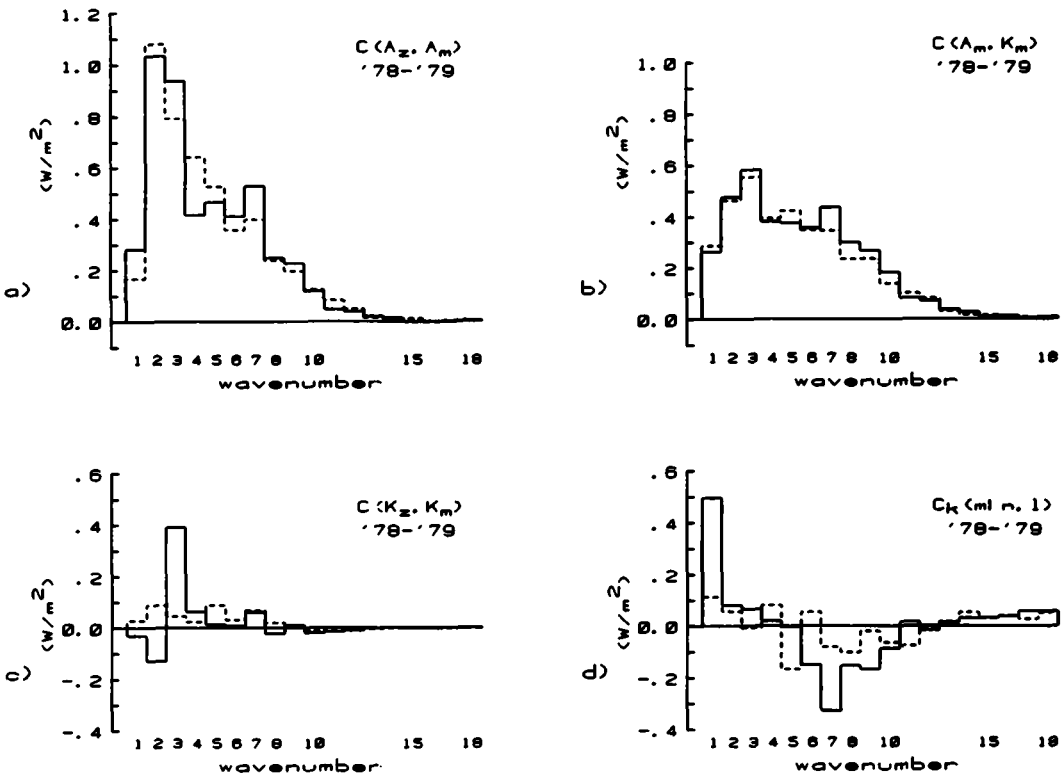


Fig. 2. 1978-79 energy budget terms: (a) $C(A_m, A_m)$; (b) $C(A_m, K_m)$; (c) $C(K_m, K_m)$; and (d) $C_K(m/n, l)$. As in Fig. 1, the solid line signifies the spectra for all blocking days and the dashed line denotes all nonblocking days. The notation is explained in the text.

(wavenumbers 1–3) is greater during blocking and no other systematic differences. The energy conversions $C(A_2, A_m)$ and $C(A_m, K_m)$ (Fig. 2a, b) are quite similar for the blocking and nonblocking samples. $C(A_2, A_m)$ shows slight increases at wavenumbers 1 and 3 during blocking with largely offsetting differences in wavenumbers 4 through 7. The increased conversion at wavenumbers 1 and 3 is totally absent when the four Atlantic cases are considered alone (not shown). The $C(A_m, K_m)$ spectrum is remarkably similar in the blocking and nonblocking situations although there are slightly larger conversions in wavenumbers 7 through 10 during blocking. $C(K_2, K_m)$ (Fig. 2c) indicates a large gain in wavenumber 3 kinetic energy due to mean flow interaction that is largely offset by reduced values at wavenumbers 1 and 2 when comparing blocking and nonblocking episodes.

The largest systematic differences between blocking and nonblocking appears in the nonlinear interaction term, $C_k(m|n, l)$ (Fig. 2d). The transfer of kinetic energy from intermediate-scale wavenumbers to the largest-scale wavenumbers takes

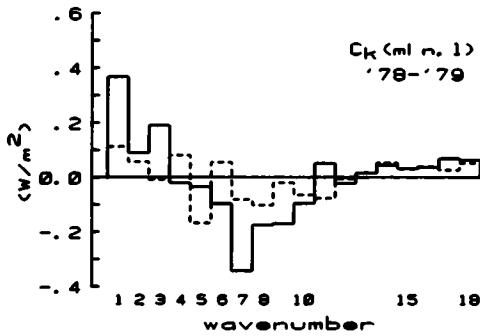


Fig. 3. $C_k(m|n, l)$ for the four Atlantic cases from 1978–79 (solid line) compared to all nonblocking days (dashed line).

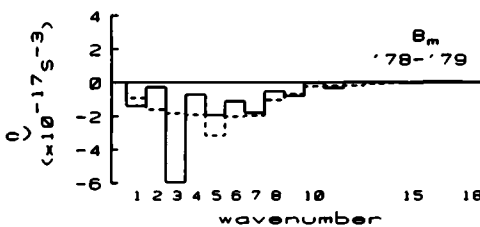
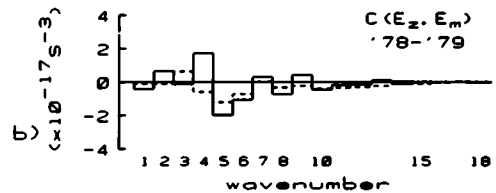
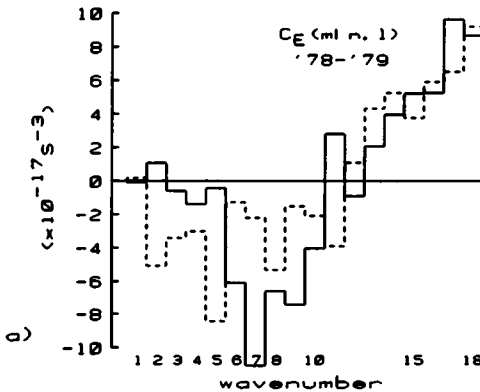


Fig. 4. The 1978–79 entropy budget terms: (a) $C_E(m|n, l)$; (b) $C(E_2, E_m)$; and (c) β_m , the rate of change of E_m due to the β effect. As in Fig. 1, the solid line represents all blocking days in the 1978–79 winter and the nonblocking results are represented by the dashed line.

place at a much greater rate during blocking periods compared to nonblocking, mostly into wavenumber 1. For the Atlantic cases alone (Fig. 3), both wavenumbers 1 and 3 benefit from the much increased kinetic energy export from wavenumbers 6 through 9 during blocking. $C_A(m|n, l)$ (not shown) is similar for the two samples and the most important boundary flux term was the horizontal flux of geopotential energy (not shown) which contributed more kinetic energy to wavenumber 1 during blocking with an offsetting loss at wavenumber 3.

The dominant term in the enstrophy budget (Fig. 4) is the nonlinear exchange term, $C_E(m|n, l)$. A very remarkable difference between blocking and nonblocking situations appears. Normally, enstrophy is cascaded from the longest waves into the shortest wavelengths (Steinberg et al., 1971). This characteristic also appears in our nonblocking sample (Fig. 4a, dashed line). However, during blocking, the net enstrophy cascade out of the longest waves (wavenumbers 1-5) disappears and a net gain of enstrophy appears at wavenumber 2. Meanwhile, the intermediate wavelengths (wavenumbers 6-10) are exporting a significantly larger amount of enstrophy than during nonblocked periods. For the Atlantic cases alone (not shown) there is an increase in enstrophy due to nonlinear interactions at both wavenumbers 2 and 3 during blocking. Thus during blocking the enstrophy cascade at low wavenumbers is reversed, as enstrophy is injected into the largest-scale waves by transient cyclone-scale waves. The only other difference in the enstrophy budgets is a greater

loss of wavenumber 3 enstrophy due to the β effect during blocking.

The differences in the nonlinear interaction terms are easily seen by comparing the kinetic energy and enstrophy flux functions for our two samples. Following Steinberg et al. (1971), these functions can be defined as

$$\frac{\delta F_k}{\delta m} = -C_k(m|n, l)$$

and

$$\frac{\delta F_E}{\delta m} = -C_E(m|n, l)$$

assuming $F_k(0) = F_E(0) = 0$. Regions of the appropriate flux function with negative slopes represent wavenumber bands gaining K or E through nonlinear interactions. Regions with positive slopes are losing energy or enstrophy. The absence of an enstrophy flux out of the lowest wavenumbers during blocking and the change in the sign of the enstrophy flux function near wavenumber 2 is evident in Fig. 5a. The much larger flux of kinetic energy into the long waves during blocking can clearly be seen in Fig. 5b. The flux functions for the Atlantic cases alone are essentially the same as those shown in Fig. 5.

3.2. 1976-77 winter

A comparison between the energy and enstrophy budgets of the December 1976 case of Atlantic blocking and the persistent, large amplitude low anomalies during January and Feb-

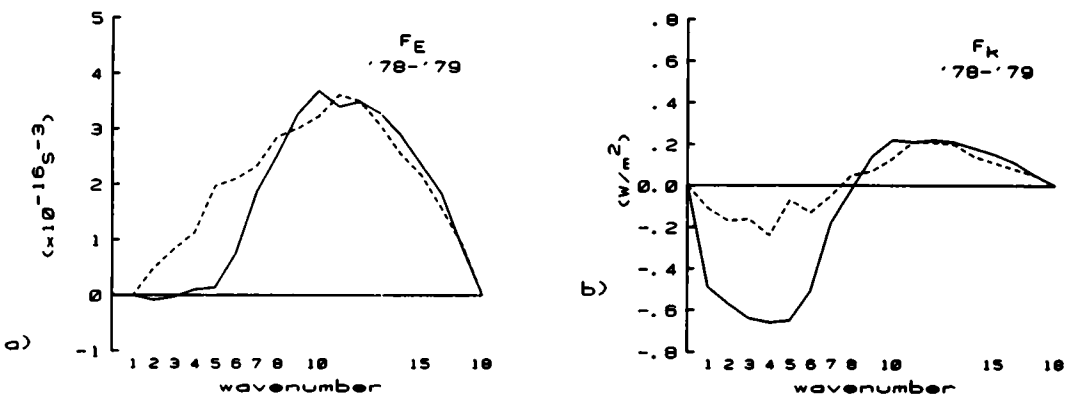


Fig. 5. The nonlinear flux functions and (a) enstrophy, F_E , and (b) kinetic energy, F_k , for blocking (solid line) and nonblocking (dashed line) for the 1978-79 winter.

ruary 1977 are given in Figs. 6–8. In general, the December 1976 event showed relatively weak large-scale (low wavenumber) baroclinic processes compared to January–February 1977 (Fig. 7a, b) (or the 1978–79 nonblocking sample), but it does exhibit the same enhanced upscale kinetic energy flux as the 1978–79 blocking cases (Fig. 7d), and a very striking reversal of the low wavenumber enstrophy cascade (Fig. 8a) at wavenumber 2. The similarity in the behavior of Rex-type blocking in two different winters lends support to the significance of this result.

However, comparing the December 1976 event to the January and February 1977 events indicates remarkable changes in the circulation between December 1976 and the following two months. There was a remarkable increase in $C(A_z, A_m)$ and

$C(A_m, K_m)$ at wavenumbers 2 and 3 during January–February 1977 (Fig. 7a, b). This characteristic was also noted by Chen and Shukla (1983) but is even more striking when compared to the December 1976 statistics. There is also a larger net gain at low wavenumbers in K_m due to $C(K_z, K_m)$ in January–February 1977 (Fig. 7c). The impression given by these results is that planetary-scale baroclinic and barotropic processes were of dominant importance in the January–February 1977 case as opposed to the case for Rex-type blocking. The nonlinear, wave-wave interactions during January–February 1977 were dominated by large energy gains for wavenumbers 1, 3 and 4 and a large loss from wavenumber 2. The kinetic energy transfer out of the intermediate-scale waves was relatively small.

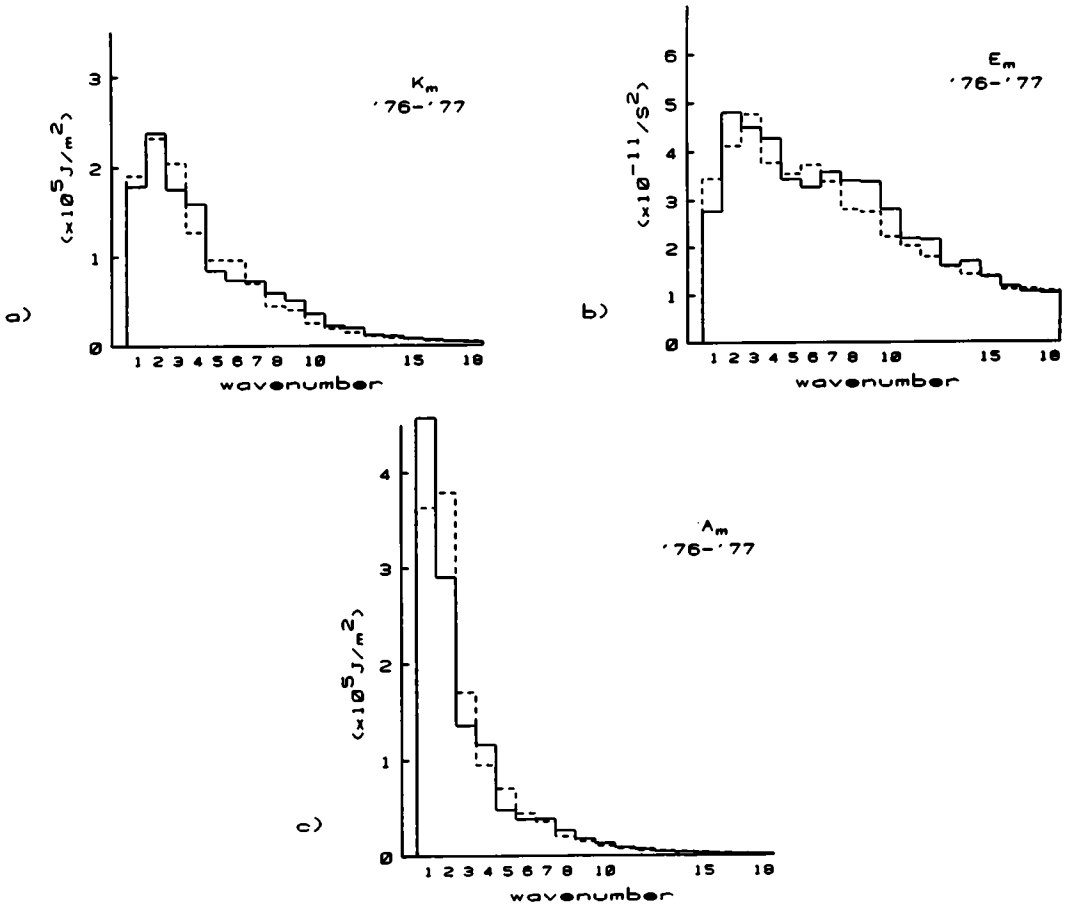


Fig. 6. Wavenumber spectra of (a) K_m ; (b) E_m ; and (c) A_m for the 1976–77 winter. Here the solid line signifies the December 1976 Atlantic blocking case and the dashed line represents the periods of large negative height anomalies in January and February 1977.

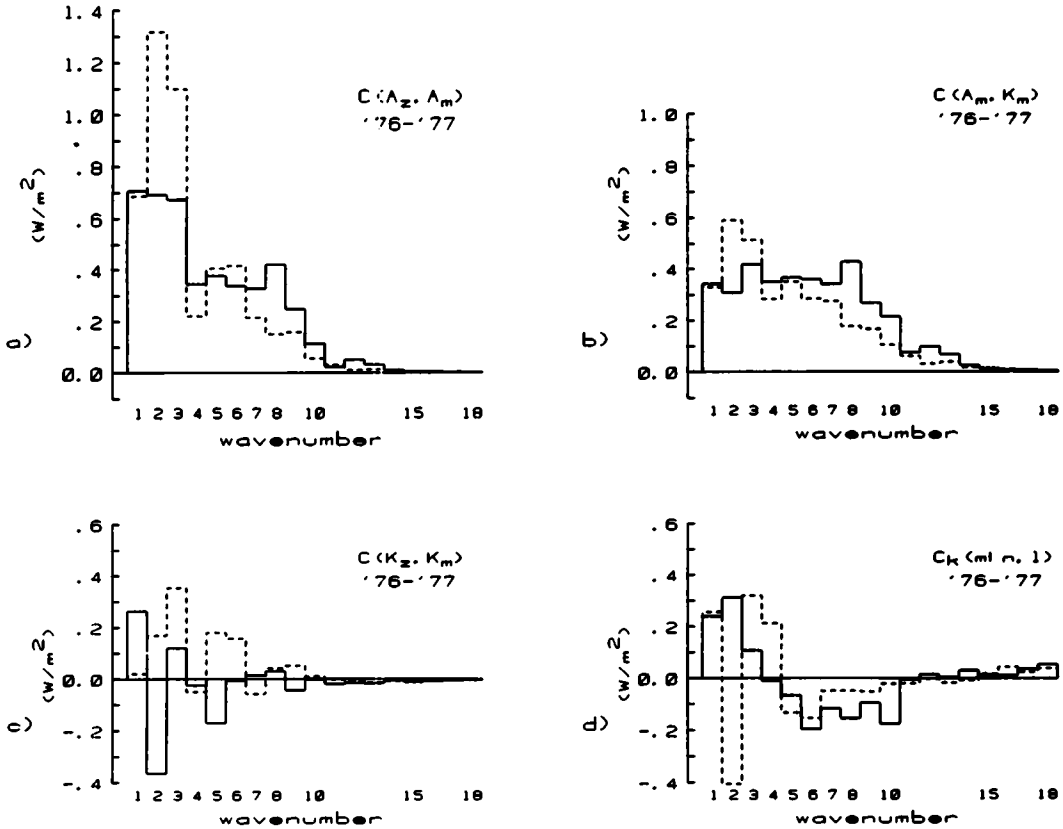


Fig. 7. (a) $C(A_z, A_m)$; (b) $C(A_m, K_m)$; (c) $C(K_z, K_m)$; and (d) $C_k(mln, l)$ for the 1976–77 winter. As in Fig. 6, the solid line represents the December 1976 blocking case and the January–February 1977 negative anomalies energetics are represented by the dashed line.

This is consistent with the reduced intermediate-scale baroclinic activity [$C(A_z, A_m)$ and $C(A_m, K_m)$ at wavenumbers 7–10 and 6–10, respectively (Fig. 7a, b)] during January–February 1977.

The nonlinear enstrophy exchange, $C_E(mln, l)$ (Fig. 8a), for the December 1976 case is similar to the 1978–79 cases as noted above (e.g., reversal of cascade at low wavenumbers and increased export of enstrophy from intermediate-scale wavenumbers), but the January–February 1977 enstrophy exchange is more like the 1978–79 nonblocking sample. These qualitative features carry over to the enstrophy and energy flux functions (Fig. 9). Notice the very striking reversal in the enstrophy flux function at low wavenumbers for the December 1976 case (Fig. 9a). Also notice the much lower value of the enstrophy flux function for

the January–February 1977 case in a nearly constant range from roughly wavenumbers 8 to 15. The enstrophy flux function in the same range for the December 1976 blocking case is virtually identical to the 1978–79 blocking and nonblocking samples.

3.3. Predictability question

The rate of error growth in numerical weather prediction models due to small-scale inaccuracies in the initialization can be related to the rate of down-scale enstrophy cascade in a constant enstrophy flux inertial subrange of a two-dimensional turbulent fluid (Leith and Kraichnan, 1972). The characteristic time of this process can be called the predictability time and is inversely proportional to the cube root of the constant rate of enstrophy transfer to higher wavenumbers in a constant

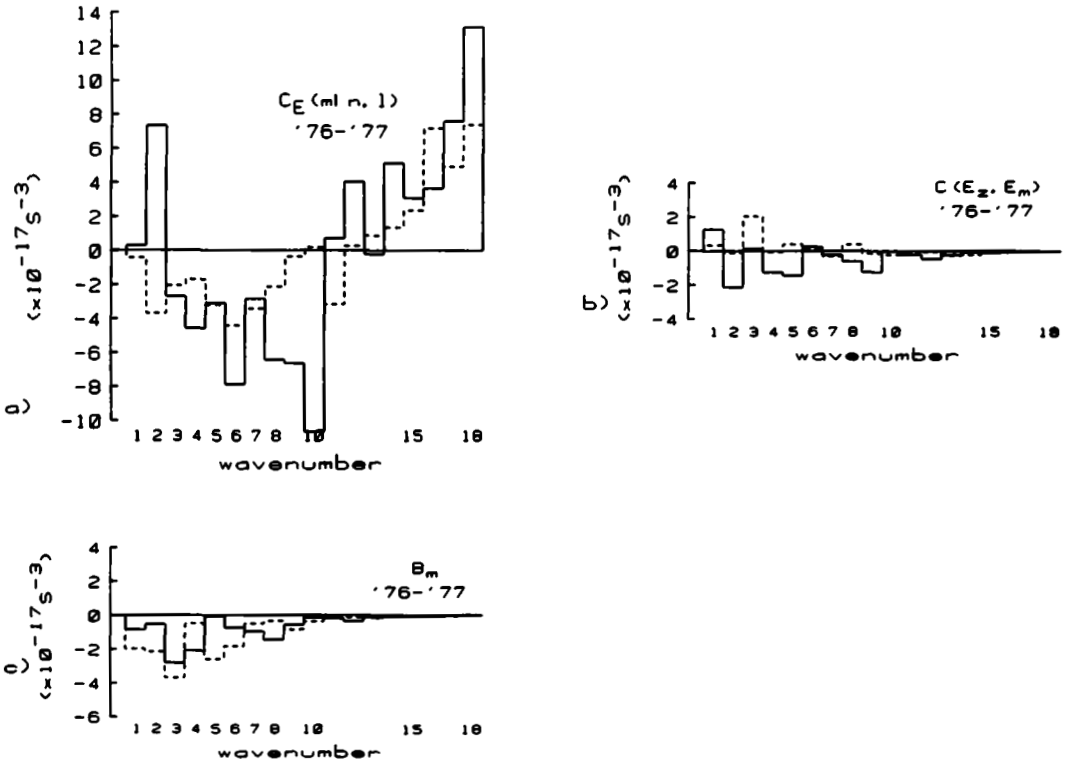


Fig. 8. The 1976-77 entrophy budget terms: (a) $C_E(ml n, l)$; (b) $C(E_z, E_m)$; and (c) B_m for the December 1976 blocking case (solid line) and the January-February 1977 negative anomaly cases (dashed line).

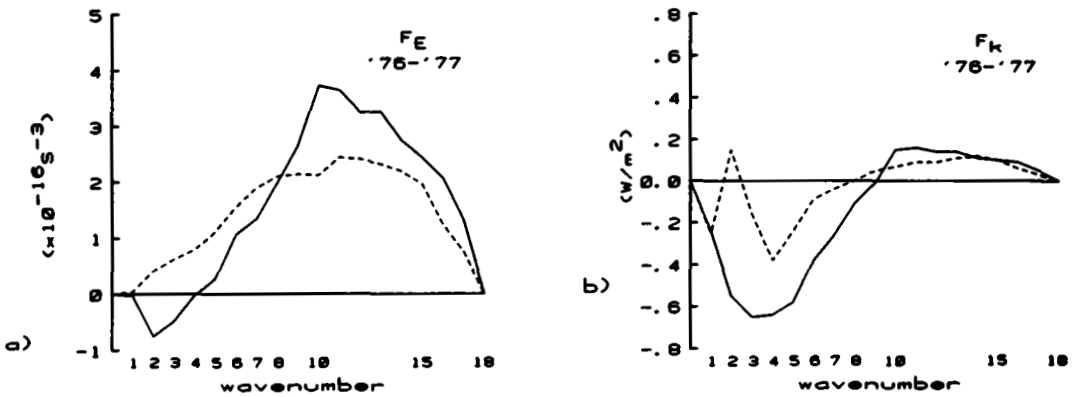


Fig. 9. The nonlinear flux functions for (a) entrophy and (b) kinetic energy for the December 1976 blocking case (solid line) and the January-February 1977 negative anomalies (dashed line).

entrophy flux inertial subrange (Lilly, 1970; Leith and Kraichnan, 1972). Although efforts to find observational evidence of a two-dimensional turbulent subrange in the atmosphere have been inconclusive (Chen and Wiin-Nielsen, 1978; Lam-

bert, 1981), the fact that the atmosphere at the larger scales behaves predominantly like a two-dimensional fluid in which the kinetic energy spectrum obeys a -3 power law (Chen and Tribbia, 1981; Julian et al., 1970; Wiin-Nielsen,

1967) suggests that a qualitative estimate of the predictability time for blocking compared to nonblocking situations based on the enstrophy flux function may be made. The estimate can only be done in a qualitative way because the numerical value of the enstrophy flux function, F_E , in the constant range is dependent upon the truncation used (Steinberg et al., 1971). The reason for this sensitivity is readily apparent from inspection of the enstrophy spectra (Fig. 1b or Fig. 6b). A finite amount of enstrophy is lost when the wavenumber expansion of the wind field is truncated at wavenumber 18. This will cause aliasing problems in the nonlinear enstrophy interaction in our truncated data set that will cause changes in the shape of the enstrophy flux function at high wavenumbers. Unfortunately, the accuracy of our data at wavenumbers higher than 18 is poor so this problem cannot be alleviated. However, we will assume the values of the flux function that we have are qualitatively correct for comparison purposes.

As noted earlier, the enstrophy flux function in the constant range is nearly identical in both blocking and nonblocking situations [Figs. 5a and 9a] suggesting no greater predictability for blocking. However, the January–February 1977 event, which was characterized by enhanced large-scale baroclinic processes, exhibited a roughly 1/3 smaller enstrophy flux rate (Fig. 9a, dashed line). This result allows us to speculate that the persistent low anomalies in 1977 were inherently more predictable than either the nonblocking or Rex-blocking cases.

An explanation of the greater predictability of the Rex-type blocking found by Bengtsson (1981) might be found in the reversal of low wavenumber enstrophy cascade (especially near wavenumber 2), and the absence of an enstrophy cascade out of the lowest 5 wavenumbers during blocking (Figs. 5a and 8a) as opposed to the normal case (Fig. 5a (dashed line) and Steinberg et al., 1971). This may indicate that the destruction of large-scale vorticity by down-scale cascade and eventual dissipation is greatly reduced or eliminated during blocking events. As a result, blocking patterns may be more persistent and therefore more predictable.

We should re-emphasize that the source of the enstrophy being cascaded into the low wavenumbers is the intermediate-scale wavenumbers. The fact that the predictability time for blocking is the same as for nonblocking may indicate that

blocking is no more predictable in the traditional sense than the cyclones that successively regenerate it.

4. Concluding remarks

To summarize, the most noteworthy differences between the spectral energy and enstrophy budgets of blocking versus nonblocking periods are in the nonlinear interaction terms. Apparently, when the ultralong waves have a large amplitude, such as during Rex-type blocking, they are able to more efficiently gain kinetic energy from the cyclone scale waves through wave–wave interactions. In addition, through a reversal of the low wavenumber enstrophy cascade, the ultralong waves are also able to gain enstrophy from the intermediate-scale waves during blocking, whereas the ultralong waves lose enstrophy through wave–wave interactions in nonblocked circumstances. The absence of enhanced large-scale baroclinic processes during the 1978–79 and December 1976 Rex-type blocking events does not augur well for the applicability to these cases of the various baroclinic blocking theories proposed recently.

The fact that the energy and enstrophy budgets for Rex-type blocking were similar in the two winters studied suggests that our findings are typical. However, our results for changes in the nonlinear interaction terms should be tested with a larger data set. This calculation is currently in progress.

The January–February 1977 negative height anomaly case presents a different class of phenomenon in which low wavenumber baroclinic energy conversions maintain the large amplitude features of the circulation and in which a significantly lower enstrophy flux function suggests greater predictability. This is in direct contrast to the Rex-type blocking cases which show no greater predictability in the traditional sense compared to nonblocking. However, the reversal of the low wavenumber enstrophy cascade does suggest a reduction in the dissipation of the low wavenumber enstrophy (assuming the atmosphere behaves like a two-dimensional turbulent fluid) and therefore greater persistence (and predictability) of the blocking pattern. In addition, the enstrophy cascade reversal may be an indication of intermittent behavior (Batchelor, 1960) in the large-scale flow

requiring no particular low wavenumber instability. (This aspect will be discussed further in a forthcoming paper.) If so, a description of blocking in terms of vortex dynamics (Batchelor, 1960; Onsager, 1949) may be useful. This possibility is being studied further.

From our results it appears that cyclone-scale waves play an important role in maintaining quasistationary blocking patterns by injecting enstrophy and kinetic energy into the large-scale flow. Bengtsson (1981) has also noted the apparent importance of transient smaller-scale waves in one case of blocking during January, 1979. Saltzman (1959) first suggested that nonlinear kinetic energy transfer from transient cyclone-scale eddies acts to maintain the quasistationary centers of action. Holopainen and Oort (1981) have suggested that in extratropical latitudes transient eddies act to maintain the enstrophy of the standing waves although more recent work disputes the

earlier result (Holopainen et al., 1982). The role of transient eddies in maintaining quasistationary features of the circulation deserves further study. Also, it would appear that theoretical models of blocking should incorporate the effects of transient eddies.

5. Acknowledgements

We would like to thank Professor B. Saltzman, Dr. G. D. Robinson, and Professor M. Ghil for their comments and suggestions. This study was supported by the National Aeronautics and Space Administration under grant NAS8—34903 at Yale University and by the National Science Foundation under grant ATM81—06034 at the Center for the Environment and Man, Inc. Computations were performed at the National Center for Atmospheric Research which is supported by the National Science Foundation.

REFERENCES

- Batchelor, G. K. (1960). *The theory of homogeneous turbulence*. Cambridge: Cambridge University Press.
- Bengtsson, L. 1981. Numerical prediction of atmospheric blocking—A case study. *Tellus* 33, 19–42.
- Bergman, K. 1979. Multivariate analysis of temperature and winds using optimum interpolation. *Mon. Wea. Rev.* 107, 1423–1444.
- Charney, J. G., Shukla, J. and Mo, K. C. 1981. Comparison of a barotropic blocking theory with observation. *J. Atmos. Sci.* 38, 762–779.
- Chen, T.-C. and Wiin-Nielsen, A. 1978. On nonlinear cascades of atmospheric energy and enstrophy in a two-dimensional spectral index. *Tellus* 30, 313–322.
- Chen, T.-C. and Tribbia, J. J. 1980. On nonlinear cascades of enstrophy over the tropics at 200 mb during two northern hemisphere summers. *Mon. Wea. Rev.* 108, 913–921.
- Chen, T.-C., Hansen, A. R. and Tribbia, J. J. 1981. A note on the release of available potential energy. *J. Meteorol. Soc. Japan* 59, 355–359.
- Chen, T.-C. and Tribbia, J. J. 1981. Kinetic energy spectra of divergent wind in the atmosphere. *Tellus* 33, 102–104.
- Chen, T.-C. and Shukla, J. 1983. Diagnostic analysis and spectral energetics of a blocking event in the GLAS climate model simulation. *Mon. Wea. Rev.* 111, 3–22.
- Dole, R. M. 1978. The objective representation of blocking patterns. In *The general circulation: Theory, modeling and observations*. Notes from a Colloquium, Summer, 1978. NCAR/CQ-6 + 1978-ASP, 406–426.
- Flattery, T. W. 1971. Spectral models for global analysis and forecasting. *Proceedings of the Sixth A.M.S. Technical Exchange Conference*, U.S. Naval Academy, 21–24 September, 1970. Air Weather Service Tech. Rep. 242.
- Hansen, A. R. and Chen, T.-C. 1982. A spectral energetics analysis of atmospheric blocking. *Mon. Wea. Rev.* 110, 1146–1165.
- Holopainen, E. O. and Oort, A. H. 1981. On the role of large-scale transient eddies in the maintenance of the vorticity and enstrophy of the time-mean atmospheric flow. *J. Atmos. Sci.* 38, 270–280.
- Holopainen, E. O., Rontu, L. and Lau, N.-C. 1982. The effect of large-scale transient eddies on the time-mean flow in the atmosphere. *J. Atmos. Sci.* 39, 1972–1984.
- Julian, P. R., Washington, W. M., Hembree, L. and Ridley, C. 1970. On the spectral distribution of large-scale atmospheric energy. *J. Atmos. Sci.* 27, 376–387.
- Lambert, S. J. 1981. A diagnostic study of global energy and enstrophy fluxes and spectra. *Tellus* 33, 411–414.
- Leith, C. E. and Kraichnan, R. H. 1972. Predictability of turbulent flows. *J. Atmos. Sci.* 29, 1041–1058.
- Lilly, D. K. 1970. Lectures in sub-synoptic scales of motions and two-dimensional turbulence. In *Dynamic meteorology* (ed. P. Morel). Dordrecht/Holland: D. Reidel Publ. Comp., 353–418.
- Miyakoda, K. and Rosati, A. 1982. The variation of sea surface temperature in 1976 and 1977. 1: The data analysis. *J. Geophys. Res.* 87, 5667–5680.

- Murakami, T. and Tomatsu, K. 1965. Energy cycle in the lower atmosphere. *J. Meteorol. Soc. Japan* 43, 73–88.
- Onsager, L. 1949. Statistical hydrodynamics. *Nuovo Cimento* 6, 3–11 (Supp.).
- Paulin, G. 1970. A study of the energetics of January 1959. *Mon. Wea. Rev.* 98, 795–809.
- Rex, D. F. 1950. Blocking action in the middle troposphere and its effect upon regional climate. II. The climatology of blocking action. *Tellus* 2, 275–301.
- Saltzman, B. 1957. Equations governing the energetics of the larger scales of atmospheric turbulence in the domain of wave number. *J. Meteorol.* 14, 513–523.
- Saltzman, B. 1959. On the maintenance of the large-scale quasi-permanent disturbances in the atmosphere. *Tellus* 11, 427–431.
- Saltzman, B. 1970. Large-scale atmospheric energetics in the wavenumber domain. *Rev. Geophys. Space Phys.* 8, 289–302.
- Steinberg, H. L., Wiin-Nielsen, A. and Yang, C. H. 1971. On nonlinear cascades in large-scale atmospheric flow. *J. Geophys. Res.* 76, 8629–8640.
- Wiin-Nielsen, A. 1967. On the annual variation and spectral distribution of atmospheric energy. *Tellus* 19, 540–559.